Synthesis

Reviews and Full Papers in Chemical Synthesis

Supporting Information

for DOI: 10.1055/a-2157-9100

Georg Thieme Verlag KG, Rüdigerstraße 14, 70469 Stuttgart, Germany

Thieme

Supporting Information

Efficient synthesis of chirally enriched 1H-imidazo [1,2-b] pyrazole and 4H-imidazo[1,2-b][1,2,4]triazole based bioactive Glycohybrids

Vinay Kumar Mishra,[a] Ghanshyam Tiwari,[a] Ashish Khanna,[a] Rajdeep Tyagi,[b] Ram Sagar[*a,b]

[a]Department of Chemistry, Institute of Science, Banaras Hindu University, Varanasi, Uttar Pradesh, 221005, India.

[b]Glycochemistry Laboratory, School of Physical Sciences, Jawaharlal Nehru University, New Delhi, 110067, India.

Email: ram.sagar@jnu.ac.in

Anti-cancer activity data

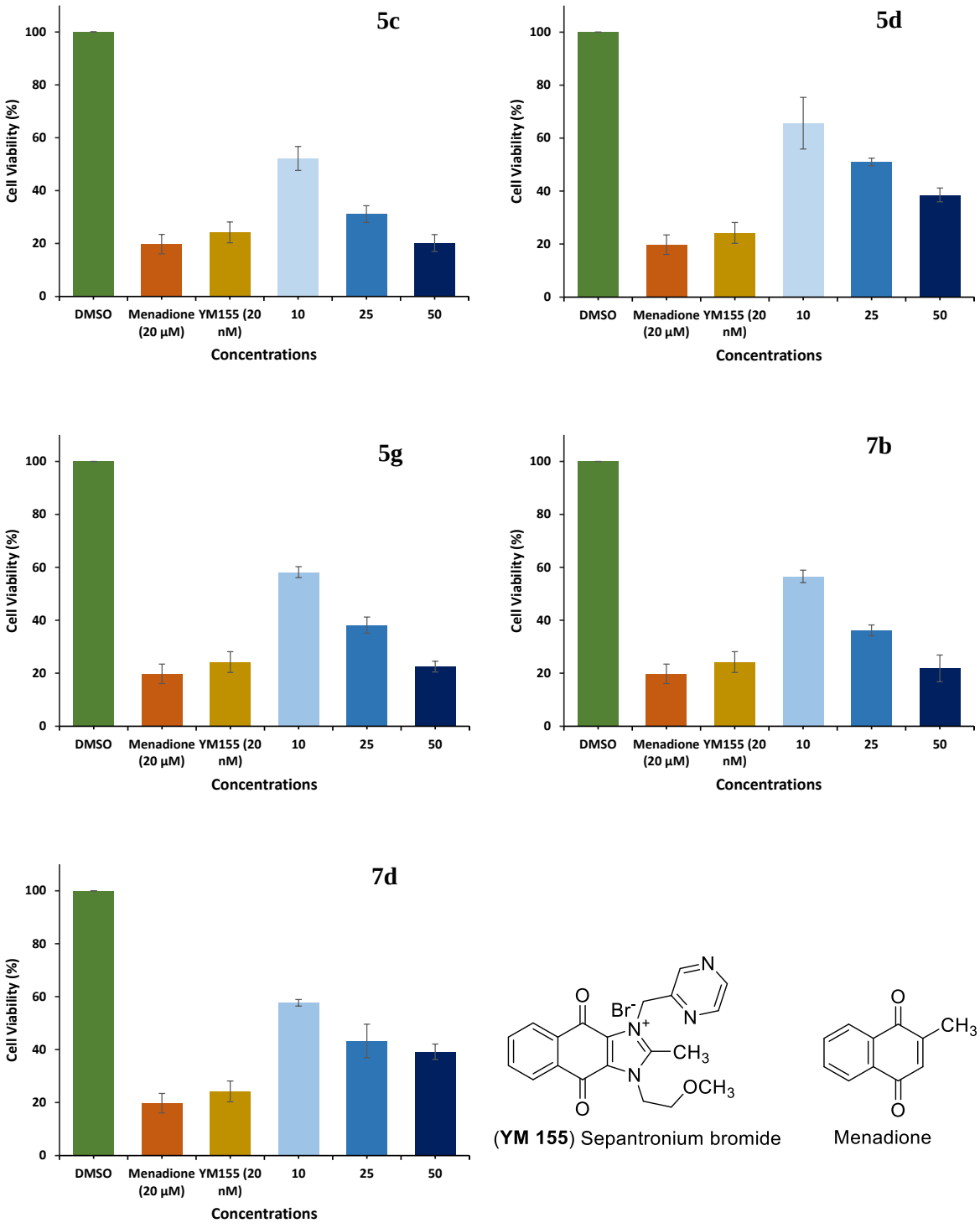

Figure S1: Anti-cancer activities in MDA-MB231 cancer cell line at different dilutions for active compounds were found at 10µM, 25µM, and 50µM for compound **5c**, **5d**, **5g**, **7b,** and **7d** respectively compared to DMSO control. Molecular structure of **YM 155** and Menadione.

The IC_{50} values for the most active compounds **5c**, **5d**, **5g**, **7b,** and **7d** were calculated against MDA-MB-231 breast cancer cell line were found 7.96, 30.9, 16.3, 14.25, and 20.74 µM respectively.To calculate half maximal inhibitory concentration (IC_{50}) of compounds **5c, 5d, 5g, 7b, and 7d**, MDA-MB-231 cells were treated for 72 h with different concentrations (10, 25 and 50µM) of the respective drugs and tested for cell viability by the MTT assay. IC_{50} values were determined by plotting values of percent cell viability against concentration of each of these compounds. The experiments were performed in triplicates, n = 3 and ± SD value was calculated for each data point. MDA-MB-231 represents a specific subtype, known as the triple negative breast cancer (TNBC).

The IC_{50} values for compound **5c, 5d, 5g, 7b** and **7d** were also calculated against MCF-7 breast cancer cells line were found 5.86, 25.42, 9.06, 6.59 and 9.63 µM respectively. While these compounds did not reach up to IC_{50} value against MDA-MB-453 cells. Furthermore, none of these compounds did have any growth inhibitory activity against normal breast epithelial cell (MCF-10A) as shown in table 3. To calculate half maximal inhibitory concentration (IC_{50}) of compounds **5c, 5d, 5g, 7b,** and **7d**, MCF-7 cells were treated for 72 h with different concentrations (1, 10 and 25 µM) of the respective drugs and tested for cell viability by the MTT assay. IC_{50} values were determined by plotting values of percent cell viability against concentration of each of these compounds. The IC_{50} values for compound **5c, 5d, 5g, 7b** and **7d** against MCF-7 breast cancer cells line were found 5.86, 25.42, 9.06, 6.59 and 9.63 µM respectively

Molecular Docking Studies

The primary objective was to evaluate the potential of newly developed glycohybrids based on imidazo [1,2-b] pyrazole and 4H-imidazo[1,2-b]triazole based glycohybrids as effective therapeutic compounds. These compounds were investigated for their various pharmacological properties, including antioxidant, anticancer, and antimicrobial activities, to optimize their use as lead compounds. One specific target of interest was the protein HCK, which belongs to the family of receptor tyrosine kinases (PTKs). HCK is involved in catalyzing the transfer of a phosphate group from ATP to specific tyrosine residues and plays a vital role in regulating various cellular signal transduction pathways, such as cell division, growth factor signaling, differentiation, survival, adhesion, migration, and invasion.

HCK, being a type of tyrosine kinase, is a crucial modulator of cancer cell invasion and metastasis. It is frequently overexpressed in solid tumors like breast, ovarian, prostate, head-and-neck, renal, pancreas, colon, and non-small-cell lung cancer. Therefore, targeting HCK

can be a promising approach for identifying potential anticancer drugs with cytotoxic properties. In order to investigate the anticancer properties of the designed imidazo[1,2-b] pyrazole and 4H-imidazo[1,2-b]triazole based glycohybrids, *in-silico* simulations were conducted between the designed compounds and the HCK protein (Human tyrosine kinase domain) (PDB ID: **1QCF**).

The active sites of protein receptors (PDB ID: **1QCF**) have been identified as LEU273, VAL281, ALA293, LYS295, ILE336, THR338, GLU339, MET341, LEU393, ALA403. These active sites or the binding domain of the target protein have been easily identified, as the target protein have co-crystallized with its inhibitor 3-phenylpyrazolopyrimidine (PP1) that binds at the ATP binding site and supress the expression of protein. The parameters of the molecule in the active region were determined with the following values: grid box sizes of 30, 30, and 32 $Å^3$, and x, y, z centers of 23.9, 28.14 and 40.85, respectively. The docking study reveals that the interaction between synthesized of imidazopyrazole and imidazotriazole based glycohybrids and catalytic site of HCK protein occurs primarily through hydrogen bonds, hydrophobic bonds, and π-stacking as shown in Figure S2.

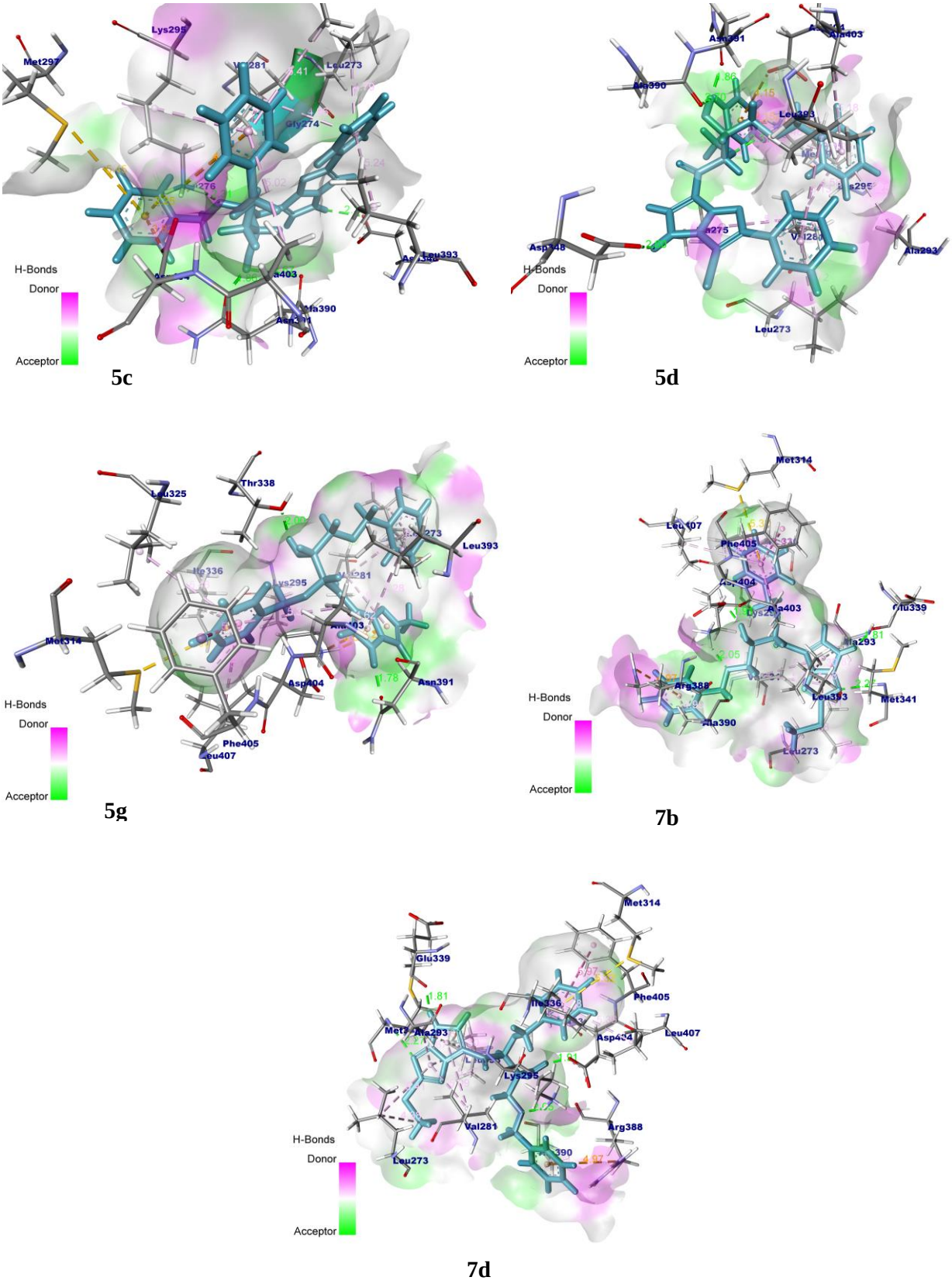

Figure S2. Docking analysis of imidazo-[1,2b]pyrazole based carbohybrids (Compounds **5c, 5d,** and **5g)** and imidazo[1,2-b]triazole based carbohybrids (Compounds **7b,** and **7d**) and catalytic site of HCK protein with 3D representation of hydrogen bond donor/acceptor surface

(shown in pink and green color), hydrogen bond (green color). The docking analysis was conducted using the collected set of compounds (blue) into the proposed binding pocket of the X-ray crystallographic structure of HCK protein (Human tyrosine kinase domain) (PDB ID: **1QCF**, resolution: 2.0 Å).

Based on the docking results, the best docking poses, docking score with high binding affinity/energies, and number of favorable interactions suggests that most of the designed imidazo [1,2-b] pyrazole and 4H-imidazo[1,2-b]triazole based glycohybrids as effective anti-cancer candidates. Among the derived library of compounds, compound **5c** displays the best docking pose with binding energy – 90.04 kcal/mol in mode 1 with minimum r.m.s.d. value and perfectly fits into the active binding pocket of protein. In Figure S4 shows 2D representation of docking results of designed imidazo-[1,2b]pyrazole based carbohybrids (Compounds **5c, 5d,** and **5g)** and imidazo[1,2-b][1,2,4]triazole based carbohybrids (**7b** and **7d**) in the binding pocket of HCK protein (PDB ID: **1QCF**). Among the library of compounds, compound **4c** displays four conventional hydrogen bonds between the LYS295, ALA390, ASP348 and ASN391 active residues, respectively. Along with this π-anion interactions have been found between the ASP404 and LYS295 active residue and phenyl ring of sugar moiety of the designed molecule. Other interactions such as π-alkyl, alkyl interactions were also found (Figure S3).

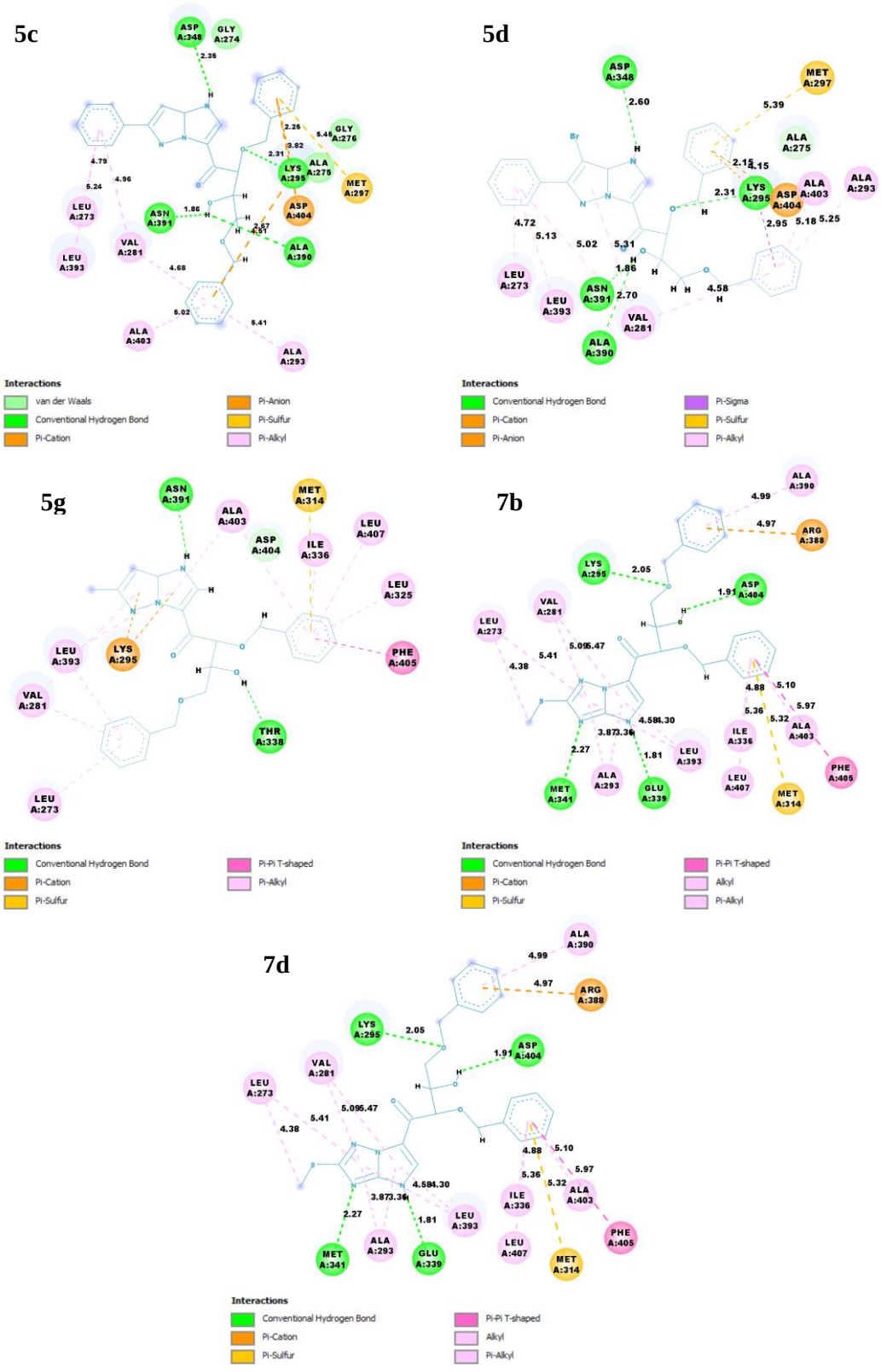

Figure S3. 2D representation of docked (Compounds **5c, 5d, 5g, 7b** and **7d)** in binding pocket of HCK protein (PDB ID: **1QCF**) displaying different interactions with ligand and amino acids.

To revalidate the docking results, our designed compound has been placed along with the co-crystallized inhibitor PP1 and visualized the binding pocket of HCK (PTKs) protein. The

results showed the overlapping structure of our designed 4H-imidazo[1,2-b]pyrazole based glycohybrid **5c** (green colour) with the co-crystallized inhibitor PP1 (yellow colour) and binds to the similar binding pocket of active residues of HCK protein (Figure S4). Also, it was found that binding energies of designed glycohybrids were more than the observed co-crystallized inhibitor PP1 of HCK protein.

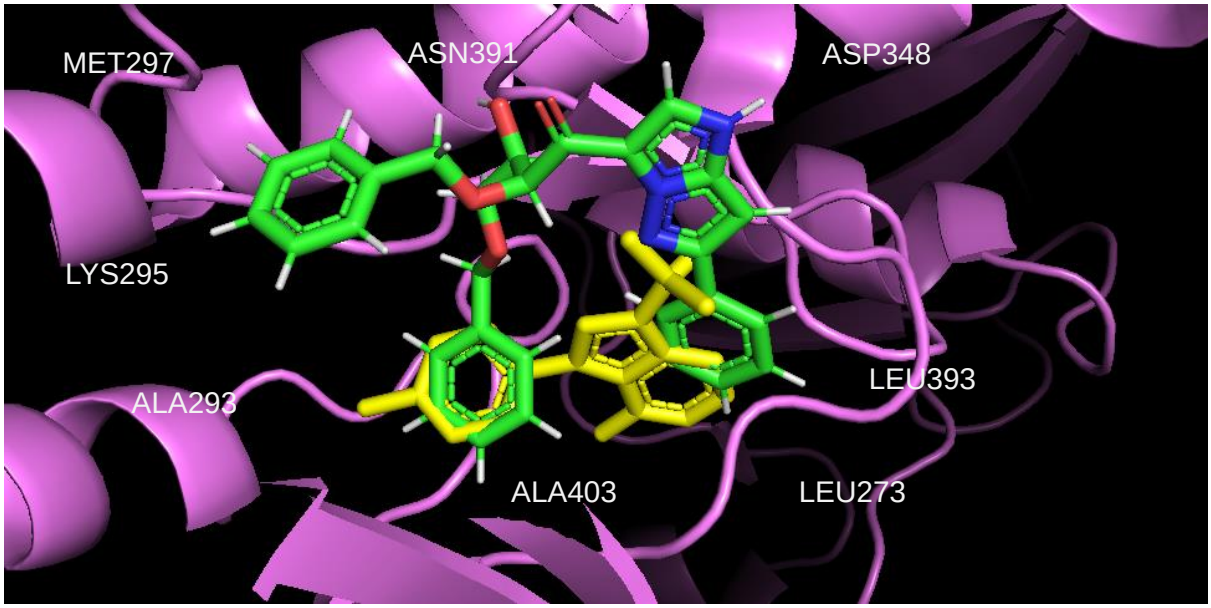

Figure S4. Overlapping of our designed compound **5c** (green) with co-crystallized inhibitor PP1 (yellow) in the binding region of HCK protein (PDB ID: **1QCF**).

Thus, results obtained from *in-silico* docking of designed molecules suggests that most of the designed molecules possess better anti-cancer activity than inhibitor PP1 and effective in inhibiting HCK (PTKs) protein and thus, validates the results obtained from *in-vitro* analysis.

Docking Analysis:

The docking studies were carried out using various derived imidazo [1,2-b] pyrazole and 4H-imidazo[1,2-b]triazole based glycohybrids with proposed binding pocket of X-ray crystallographic structure (PDB ID: **1QCF**, resolution: 2.0 Å). Docking was performed using Autodock Vina 4.0 and Schrödinger Maestro tool (Glide), and the interaction between the ligands and protein after docking was visualized and analyzed using PyMol software. The Biovia Discovery Studio Visualizer v20.1.0.19295 was used for 2D visualization and detailed ligand interaction visualization

Copies of ^{1}H NMR and ^{13}C NMR spectra of all compounds

^{1}H-NMR (500 MHz, $CDCl_3$) and ^{13}C NMR (126 MHz, $CDCl_3$)

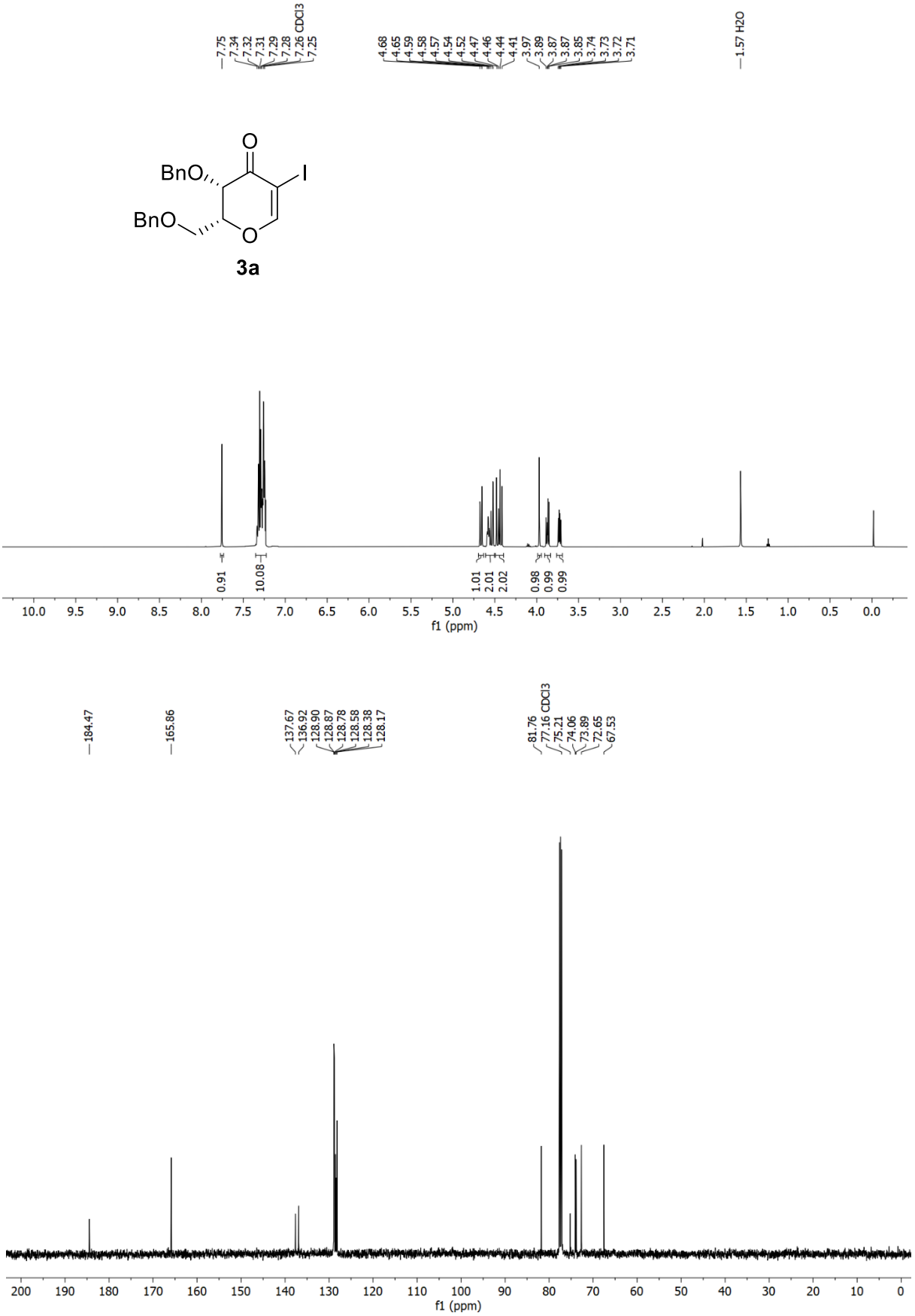

^{1}H-NMR (500 MHz, $CDCl_3$) and ^{13}C NMR (126 MHz, $CDCl_3$)

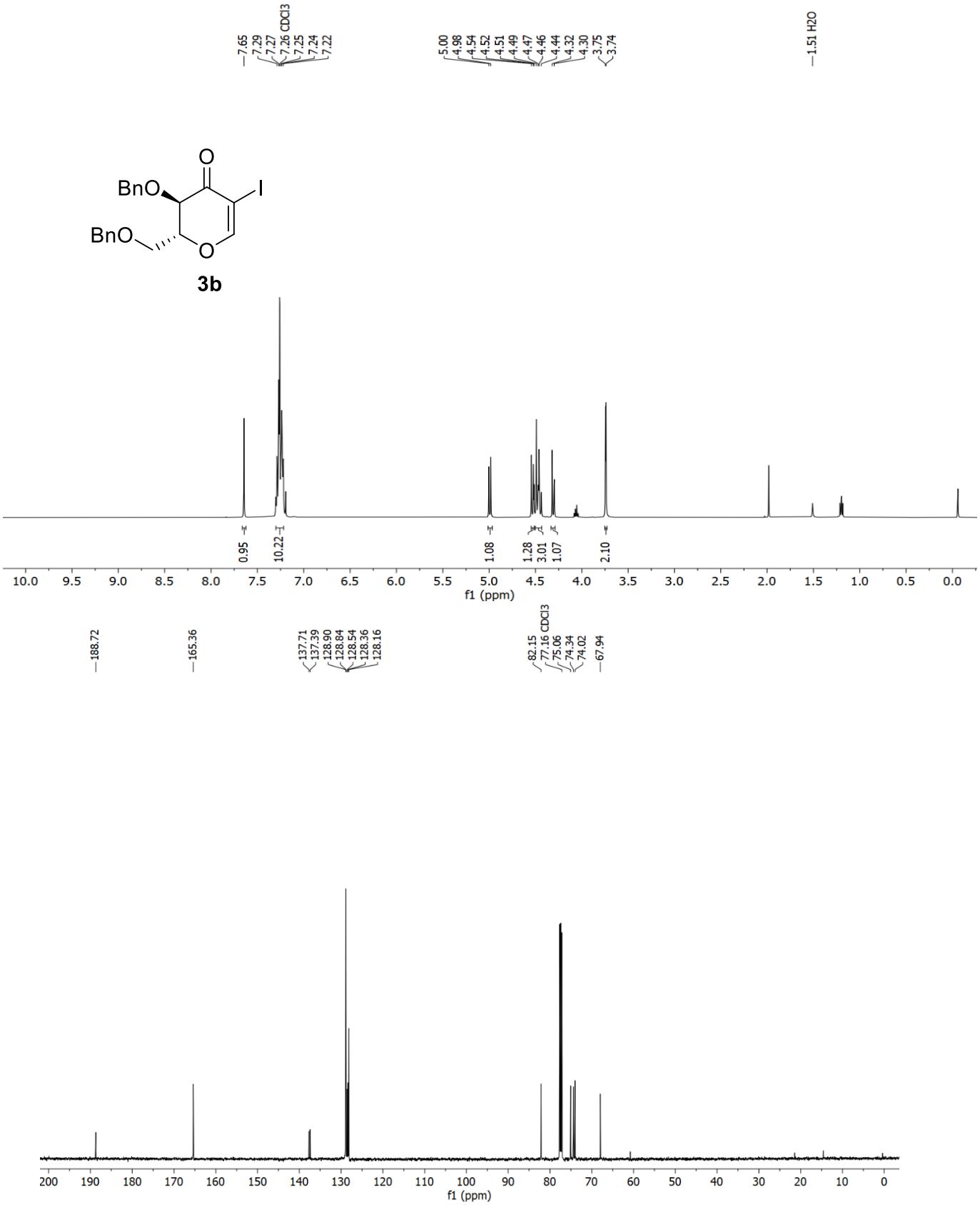

^{1}H-NMR (500 MHz, DMSO-d_6) and ^{13}C NMR (126 MHz, DMSO-d_6)

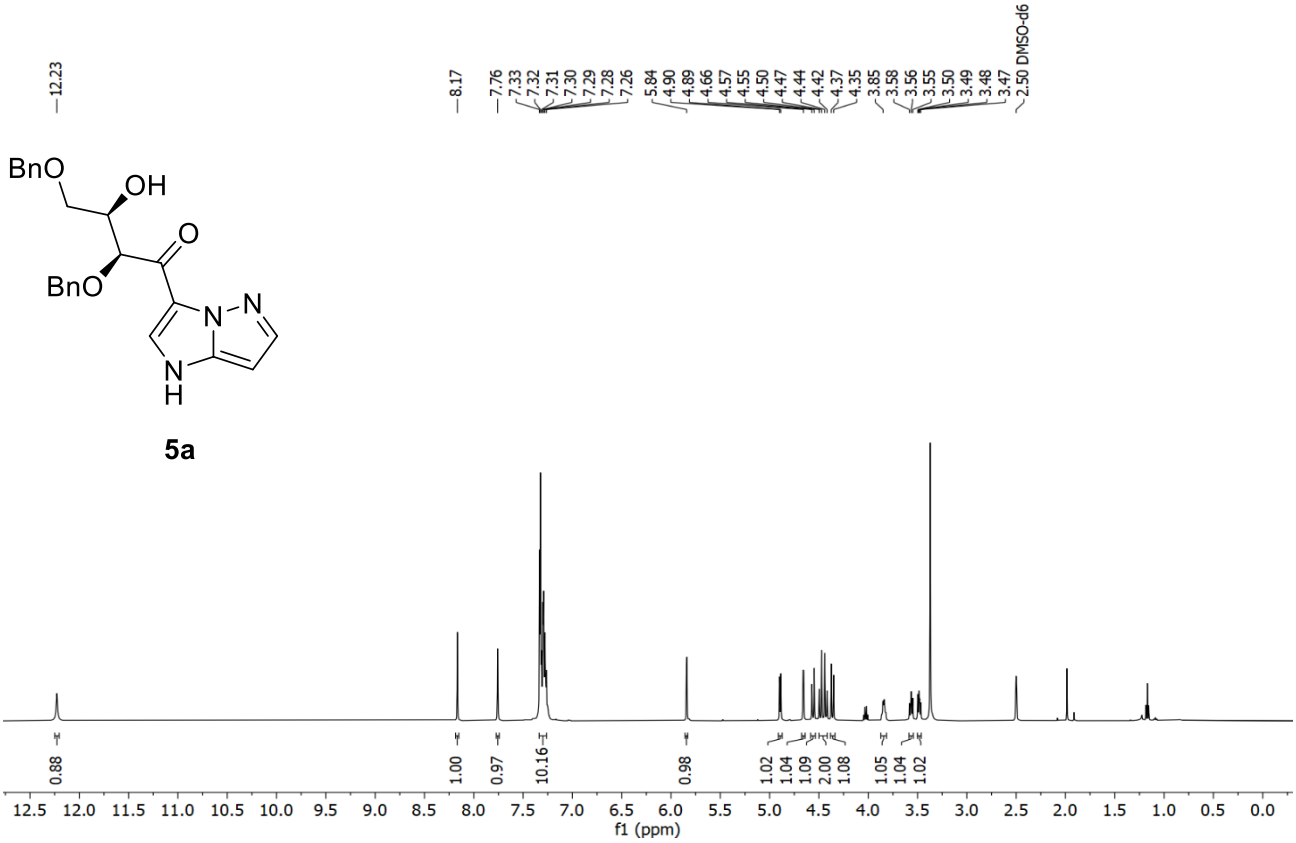

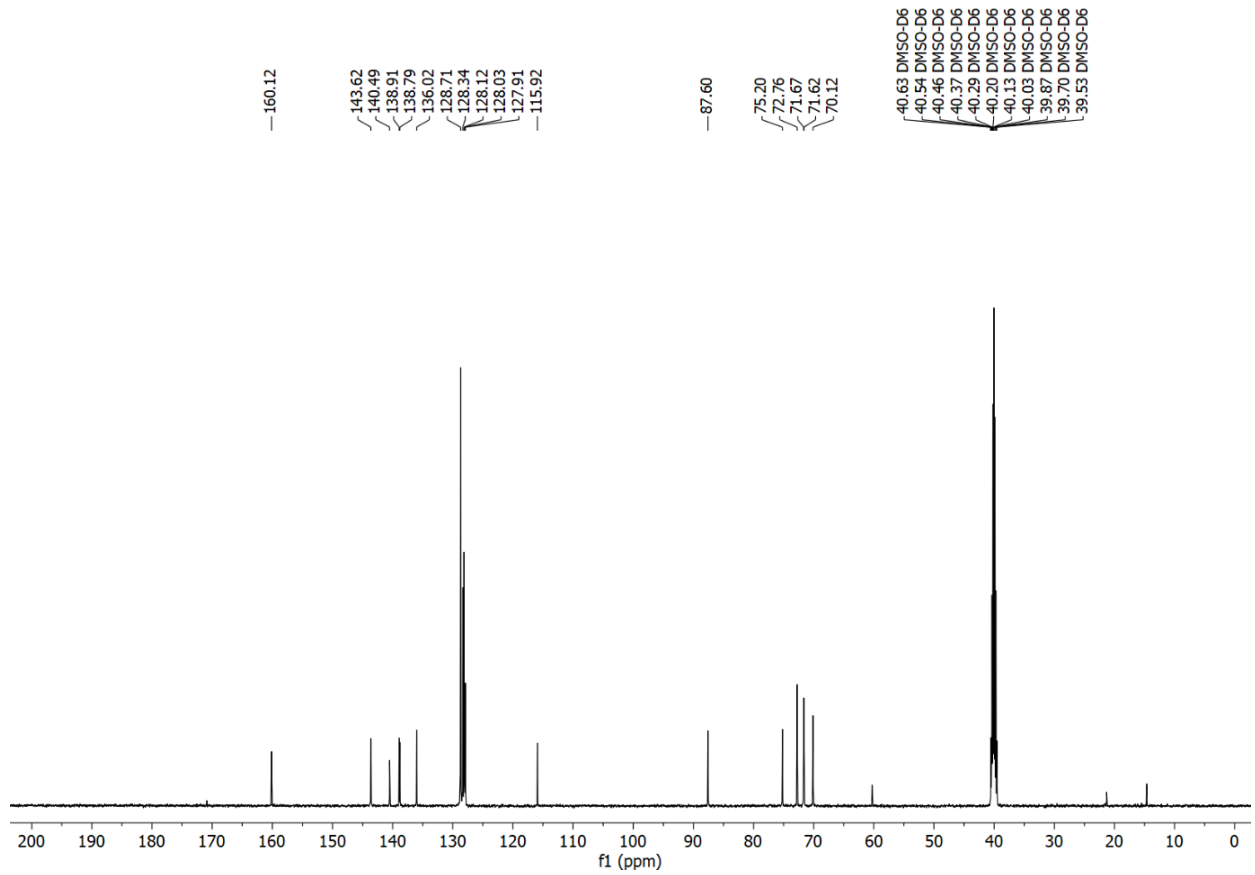

DEPT-135 (500 MHz, DMSO-d_6) **5a**

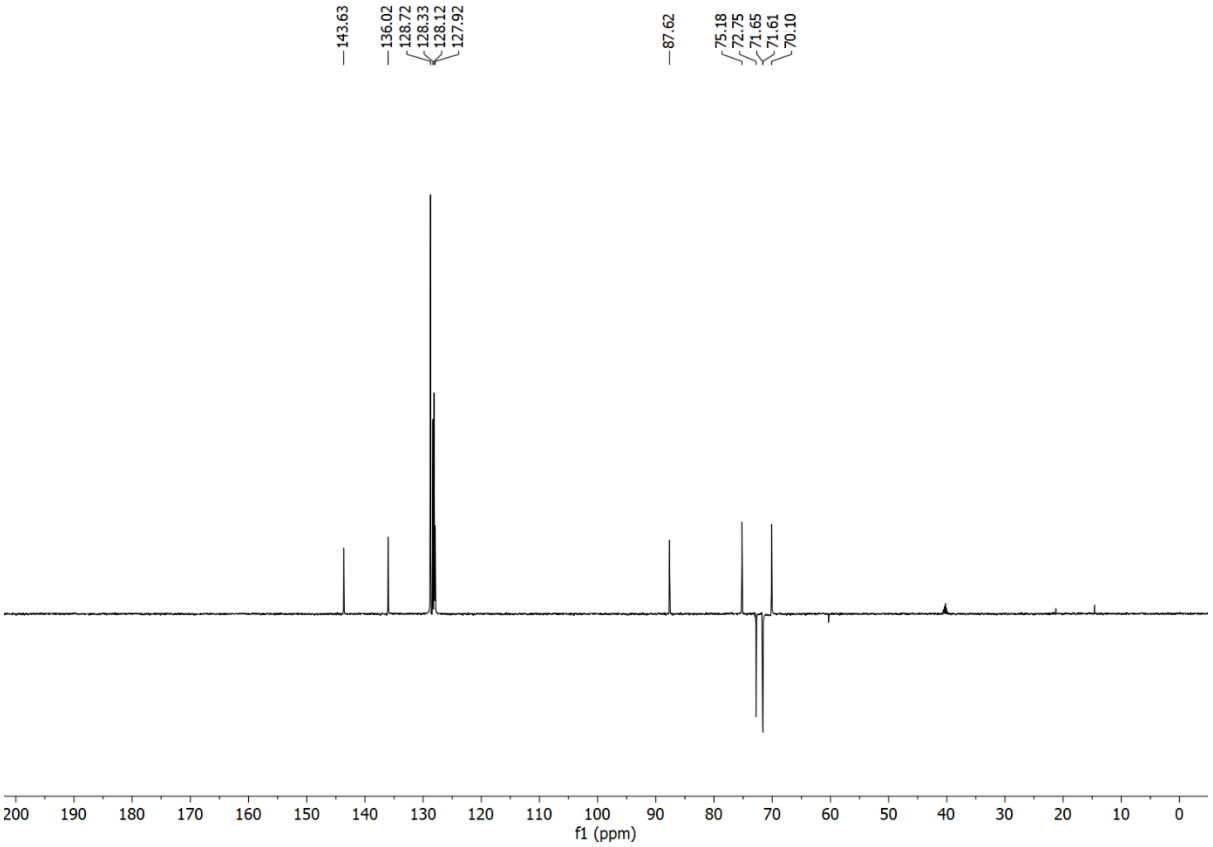

HSQC (500 MHz, DMSO-d_6) **5a**

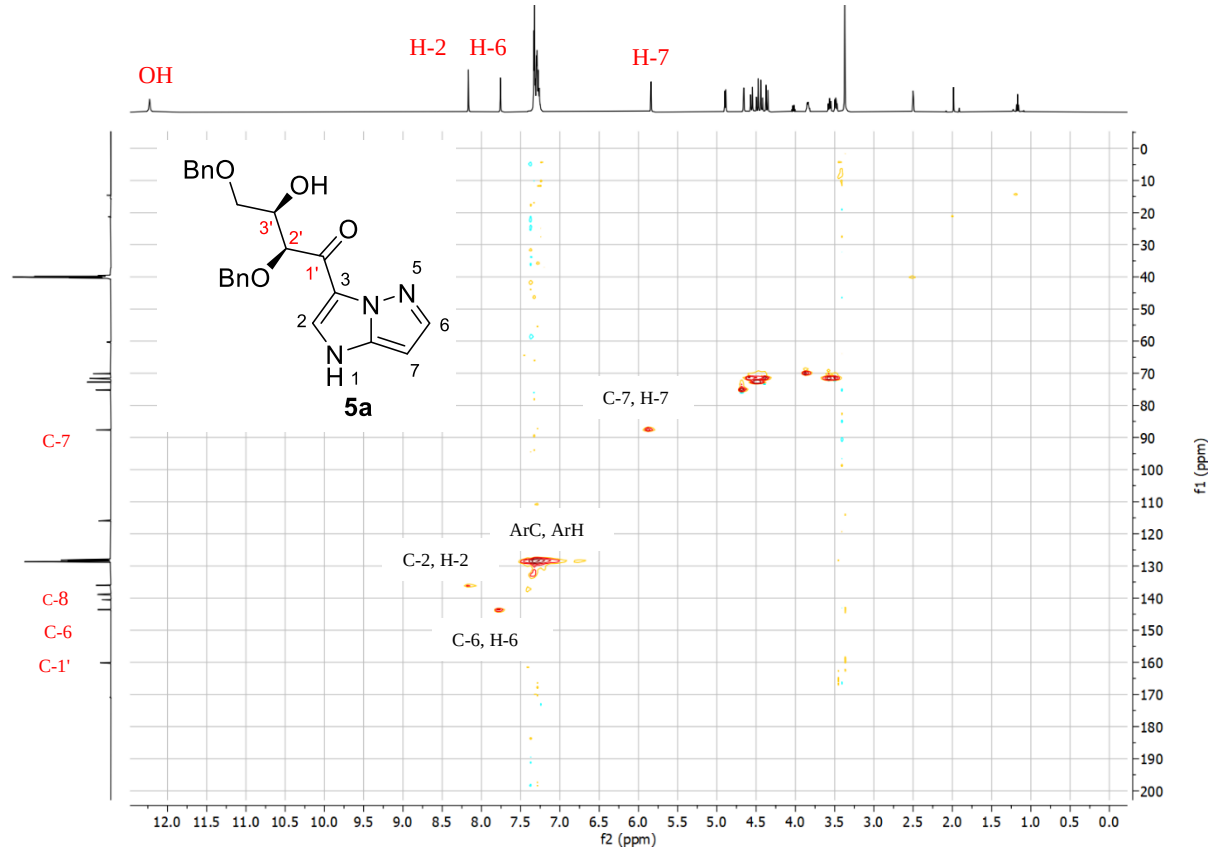

HMBC (500 MHz, DMSO-d_6) **5a**

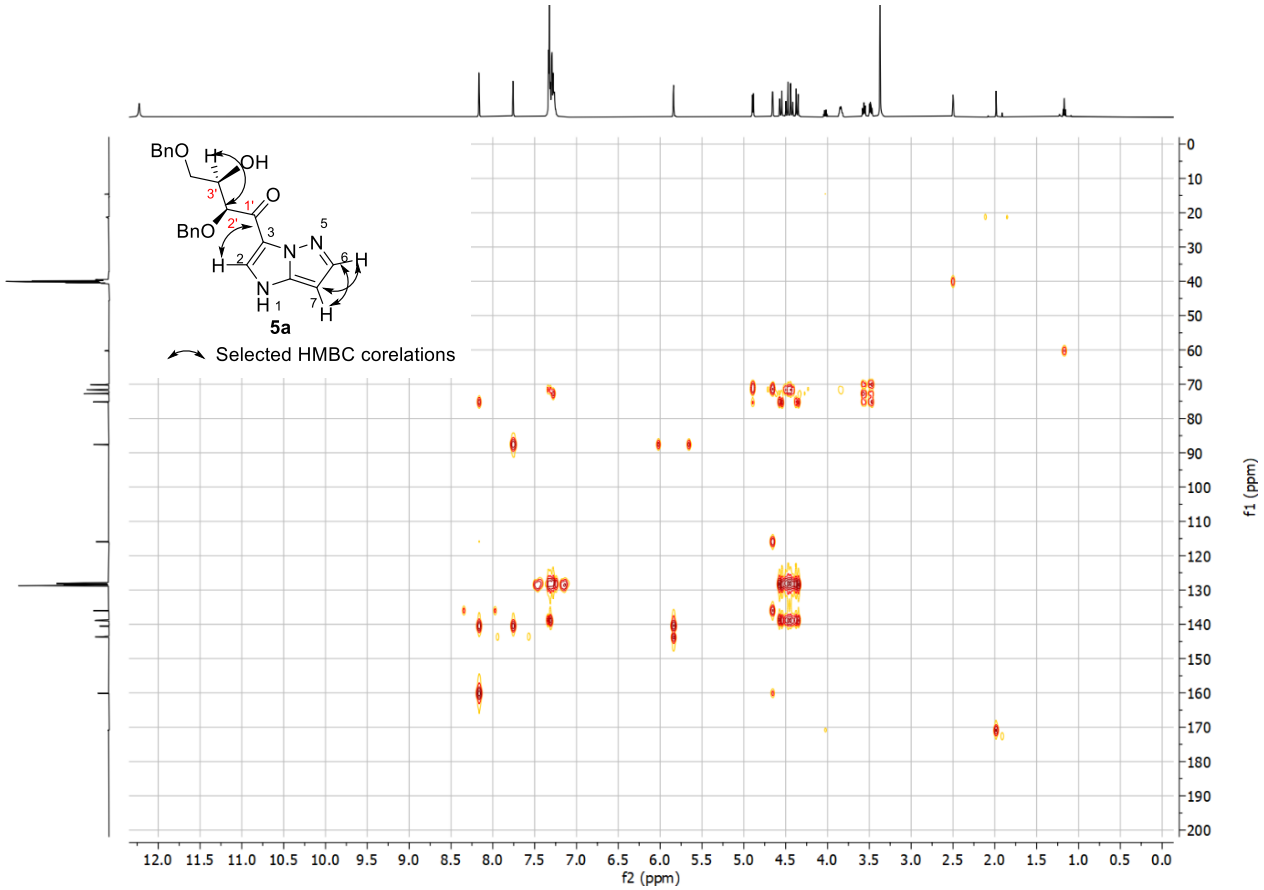

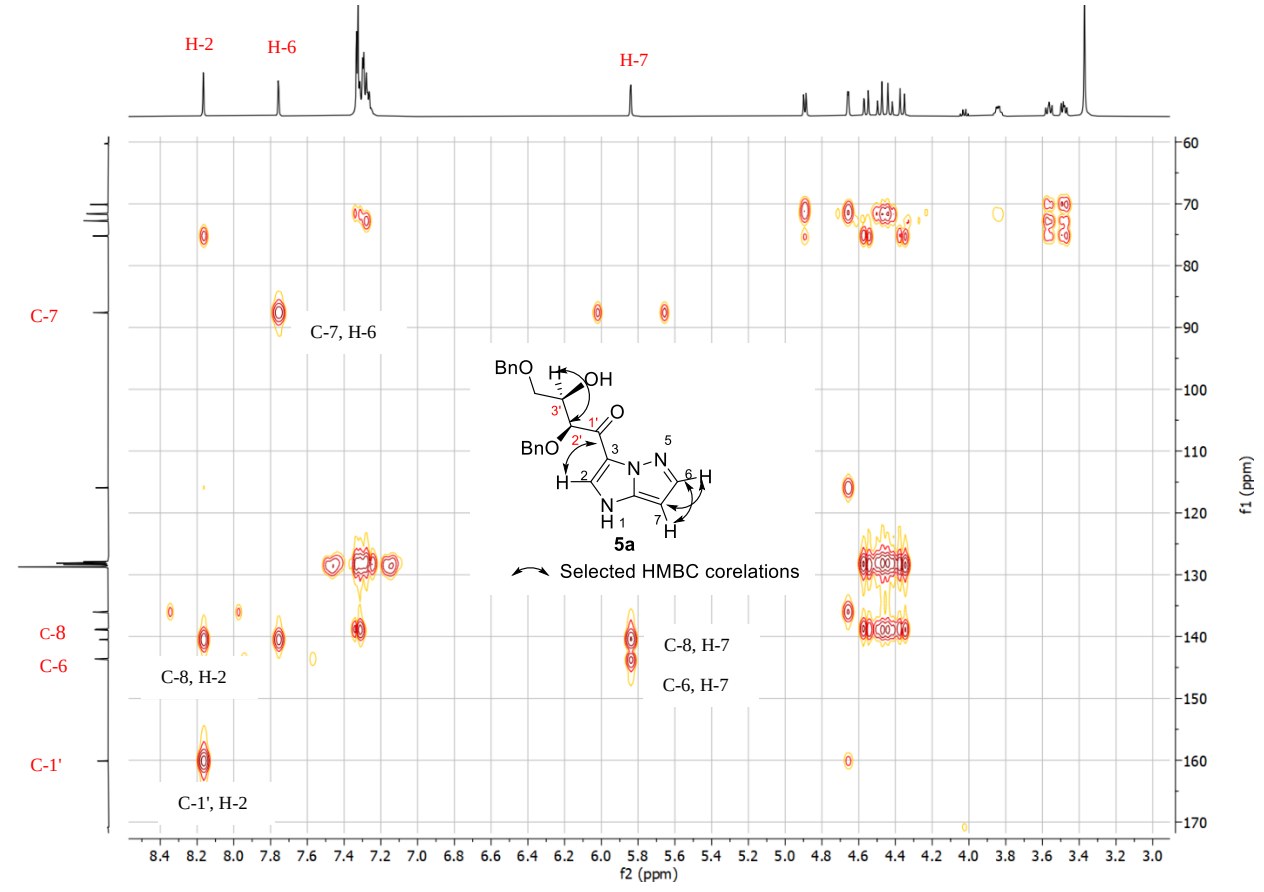

^{1}H-NMR (500 MHz, $CDCl_3$) and ^{13}C NMR (126 MHz, $CDCl_3$)

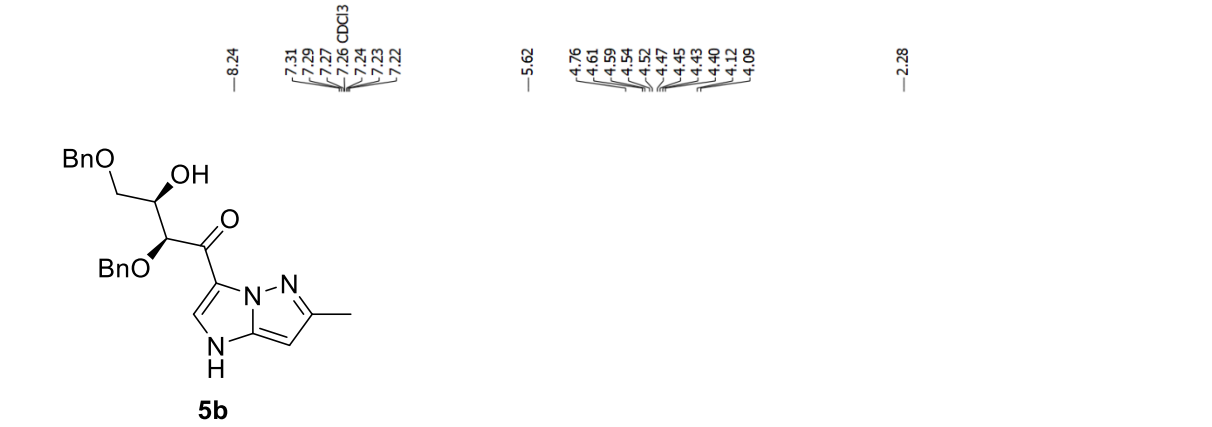

5b

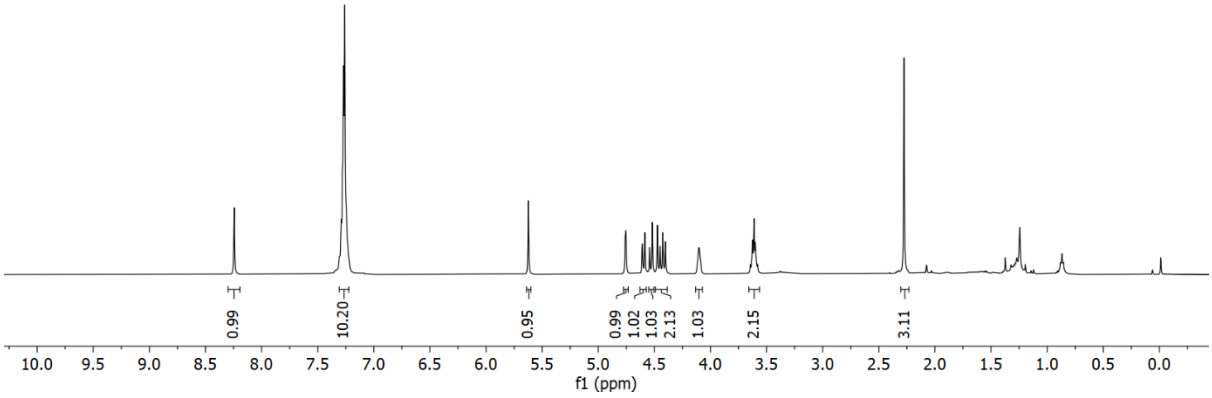

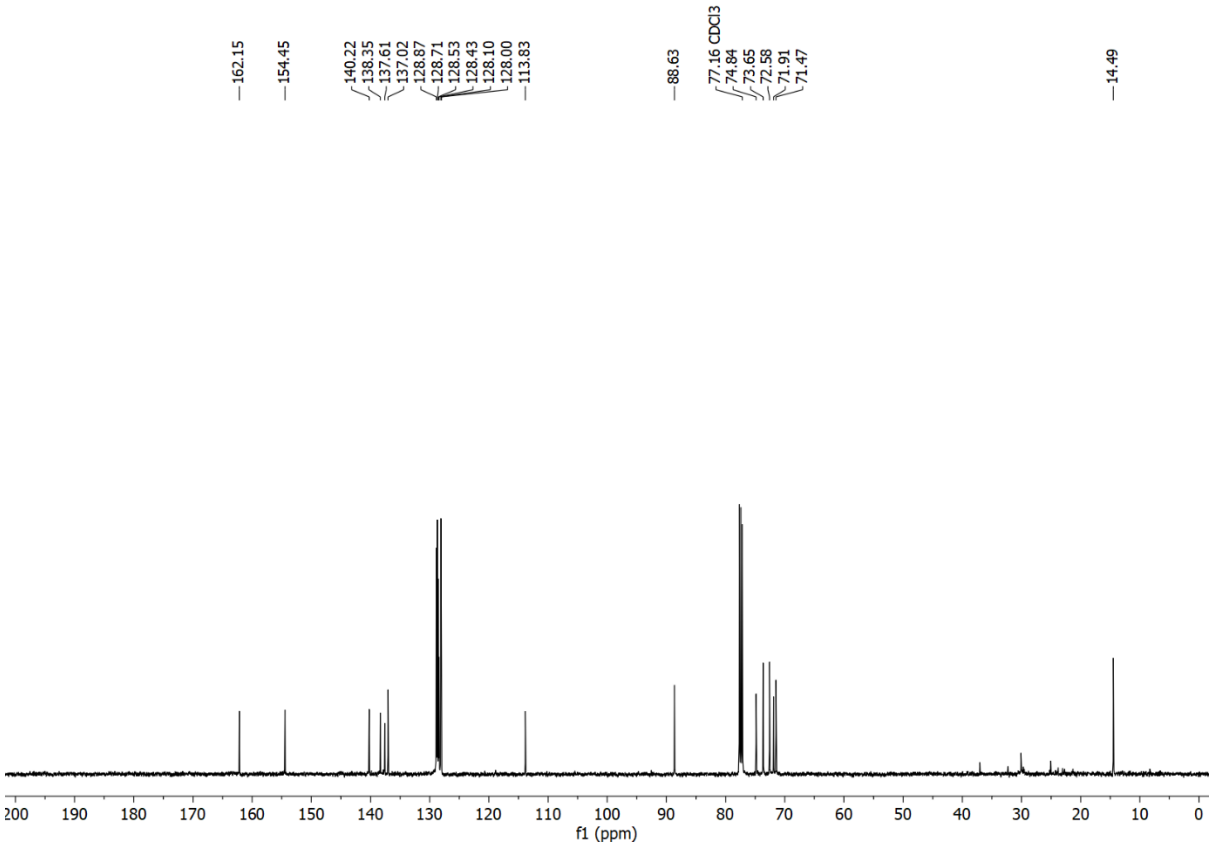

^{1}H-NMR (500 MHz, $CDCl_3$) and ^{13}C NMR (126 MHz, $CDCl_3$)

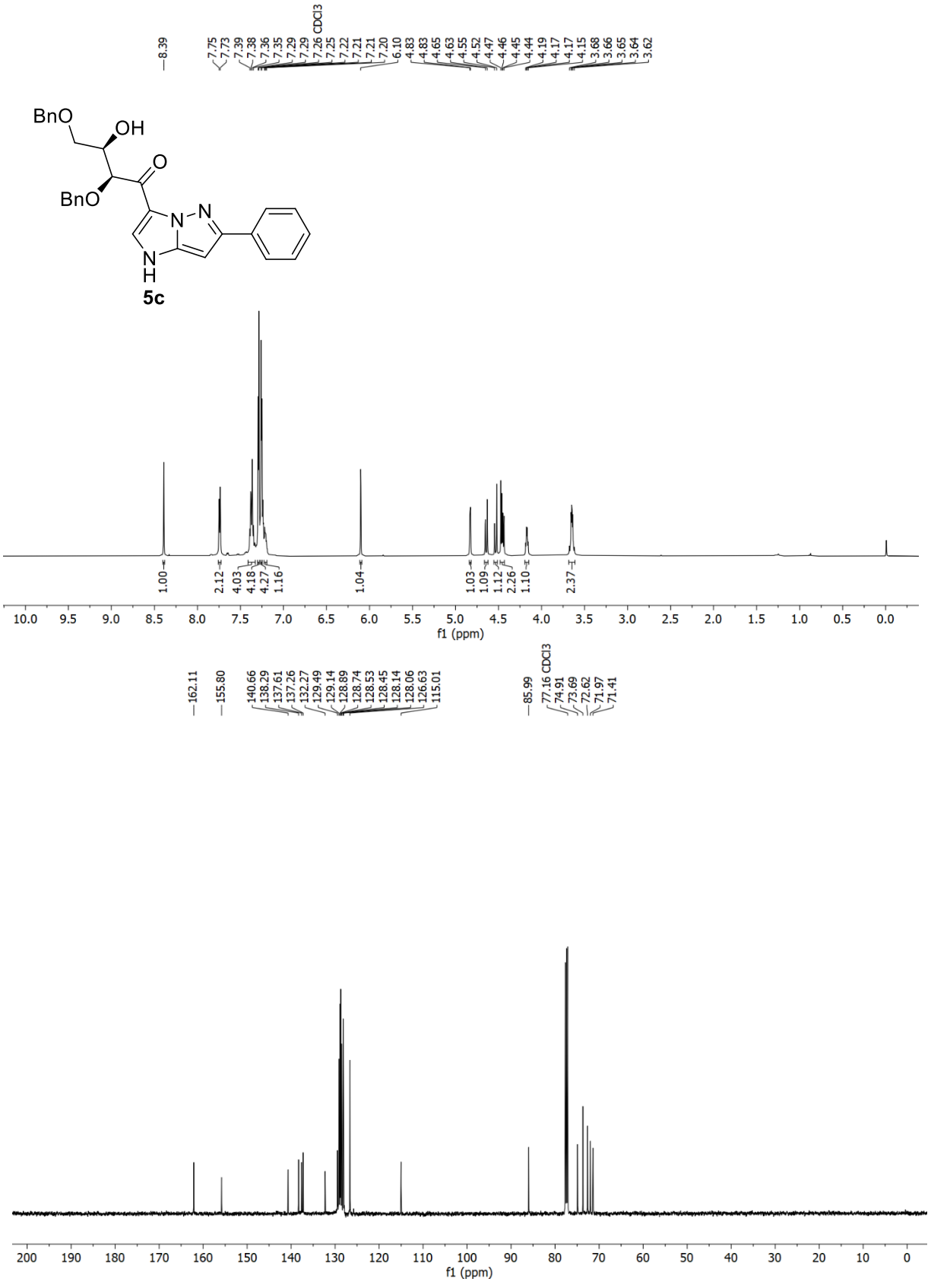

^{1}H-NMR (500 MHz, $CDCl_3$) and ^{13}C NMR (126 MHz, $CDCl_3$)

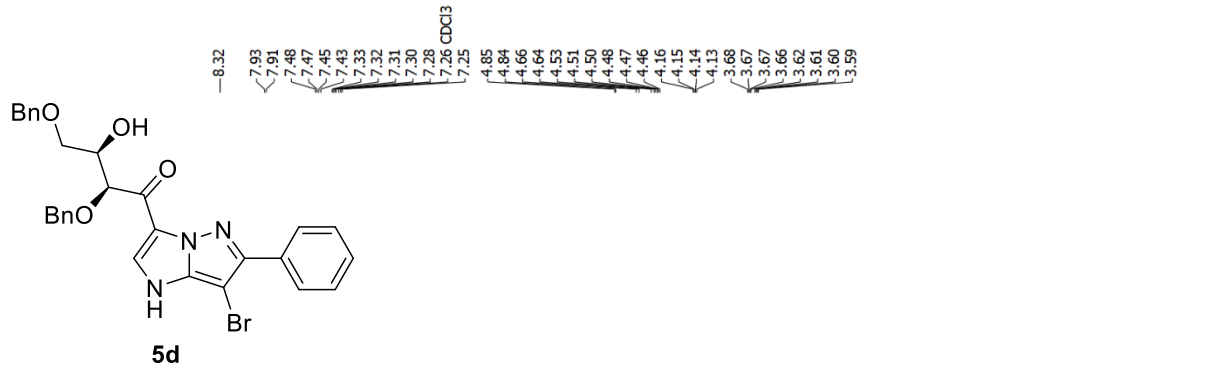

5d

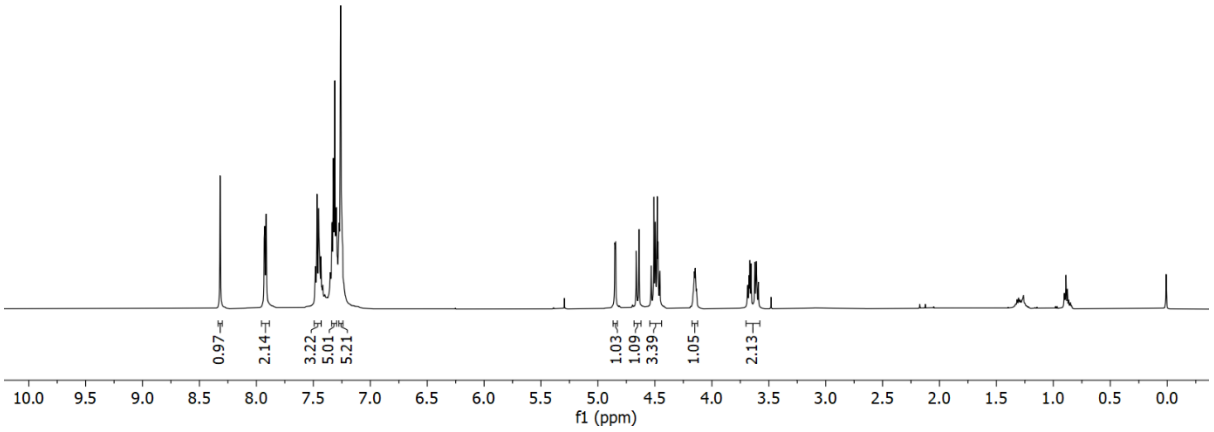

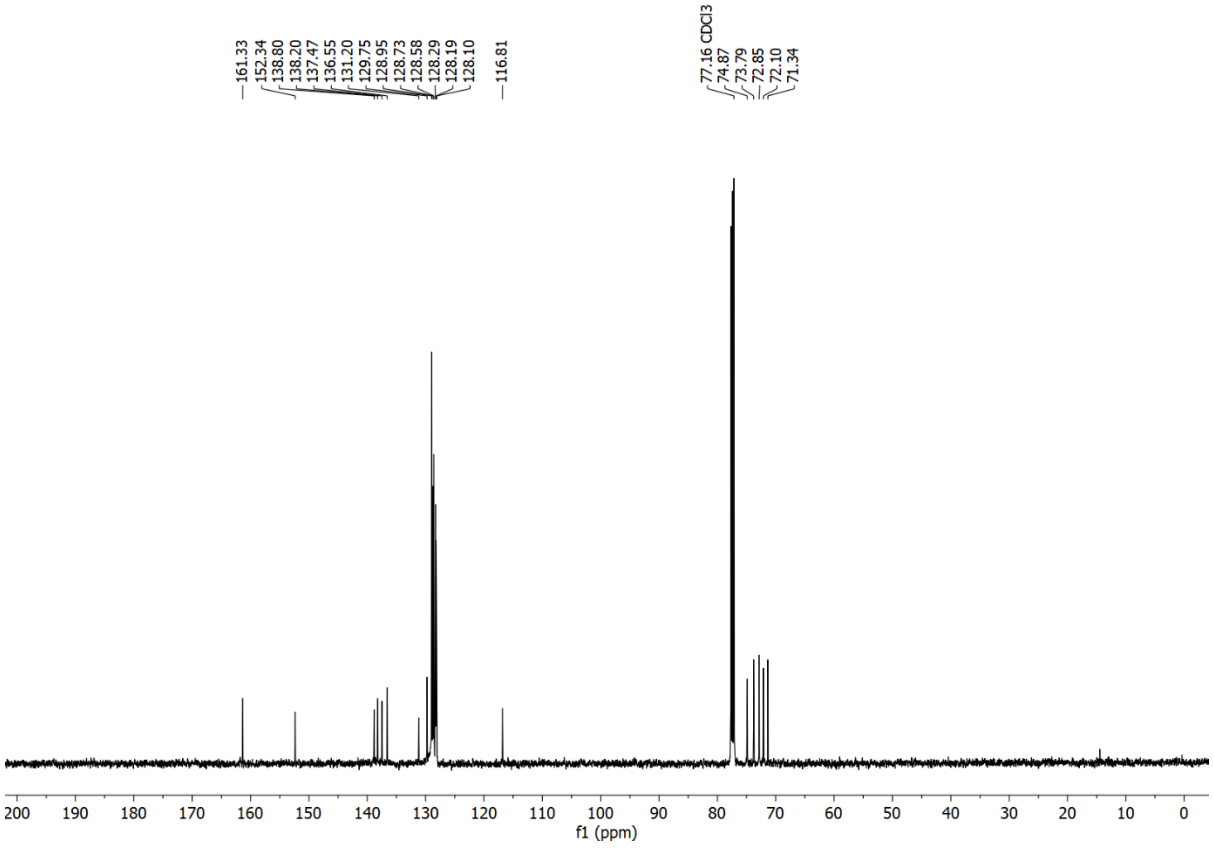

^{1}H-NMR (500 MHz, $CDCl_3$) and ^{13}C NMR (126 MHz, $CDCl_3$)

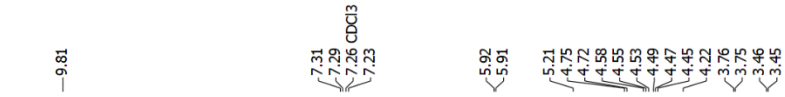

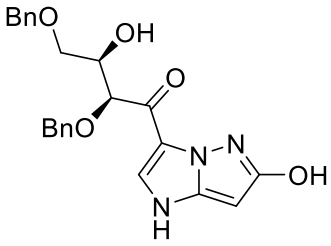

5e

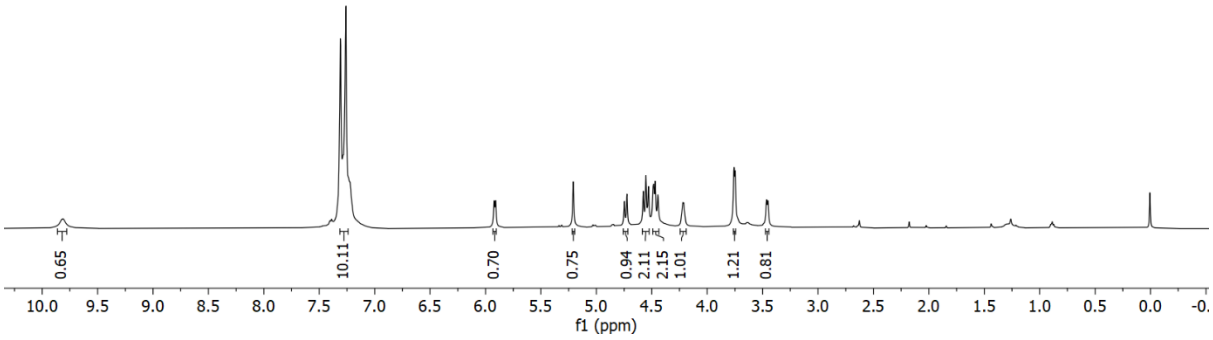

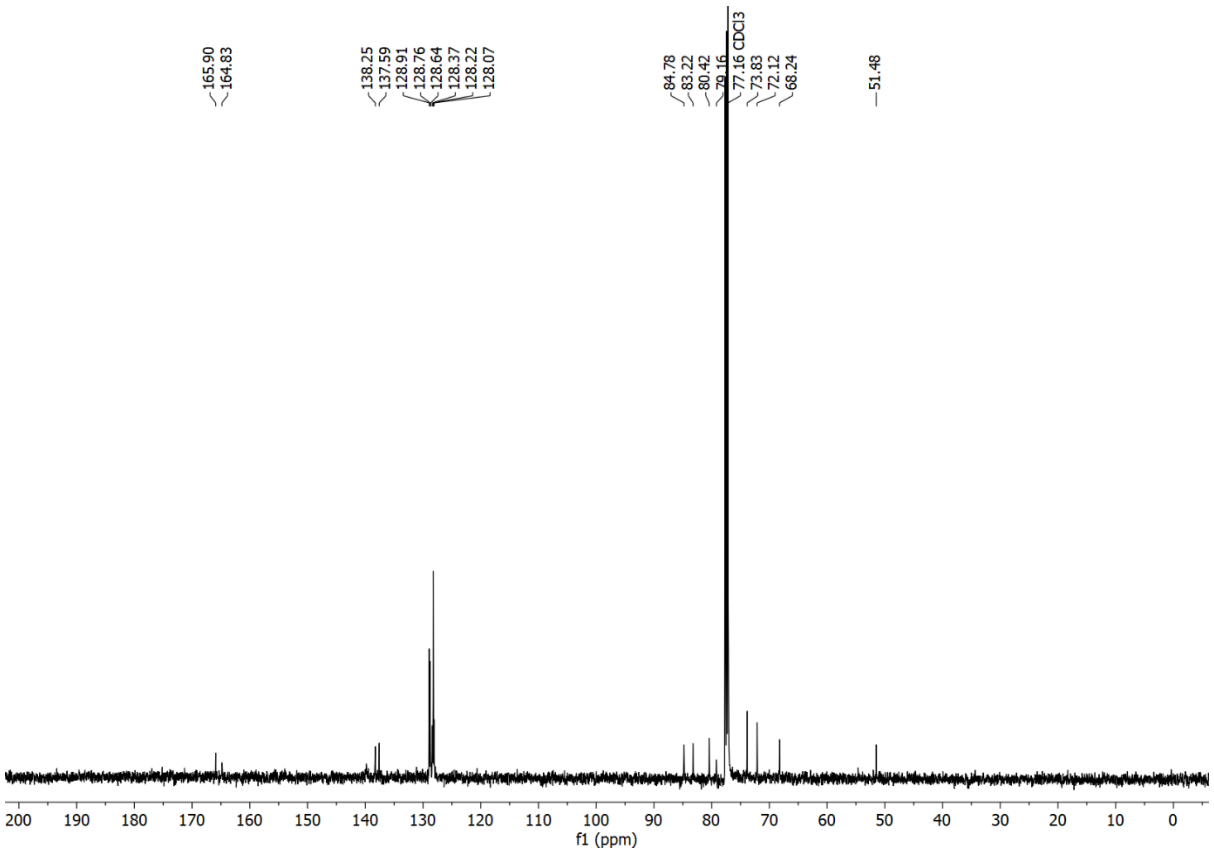

^{1}H-NMR (500 MHz, $CDCl_3$) and ^{13}C NMR (126 MHz, $CDCl_3$)

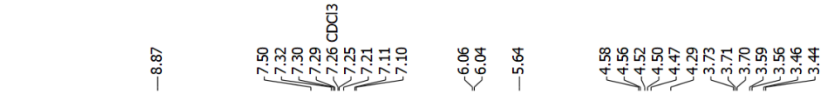

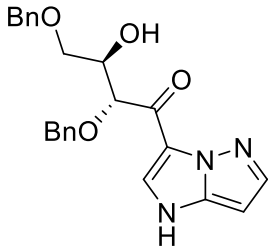

5f

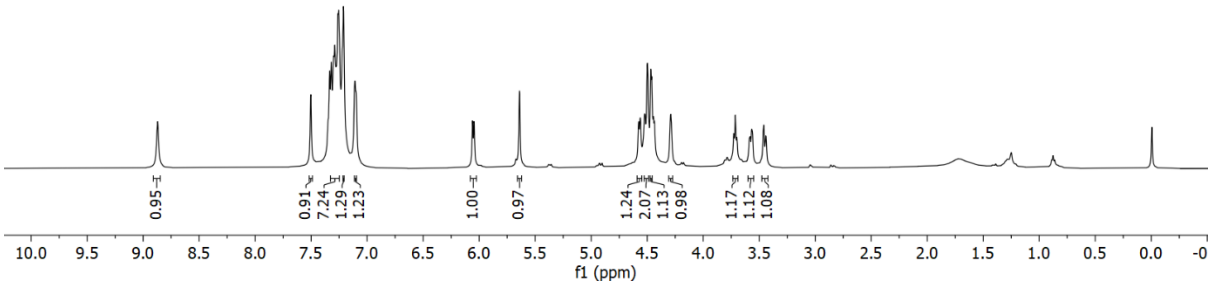

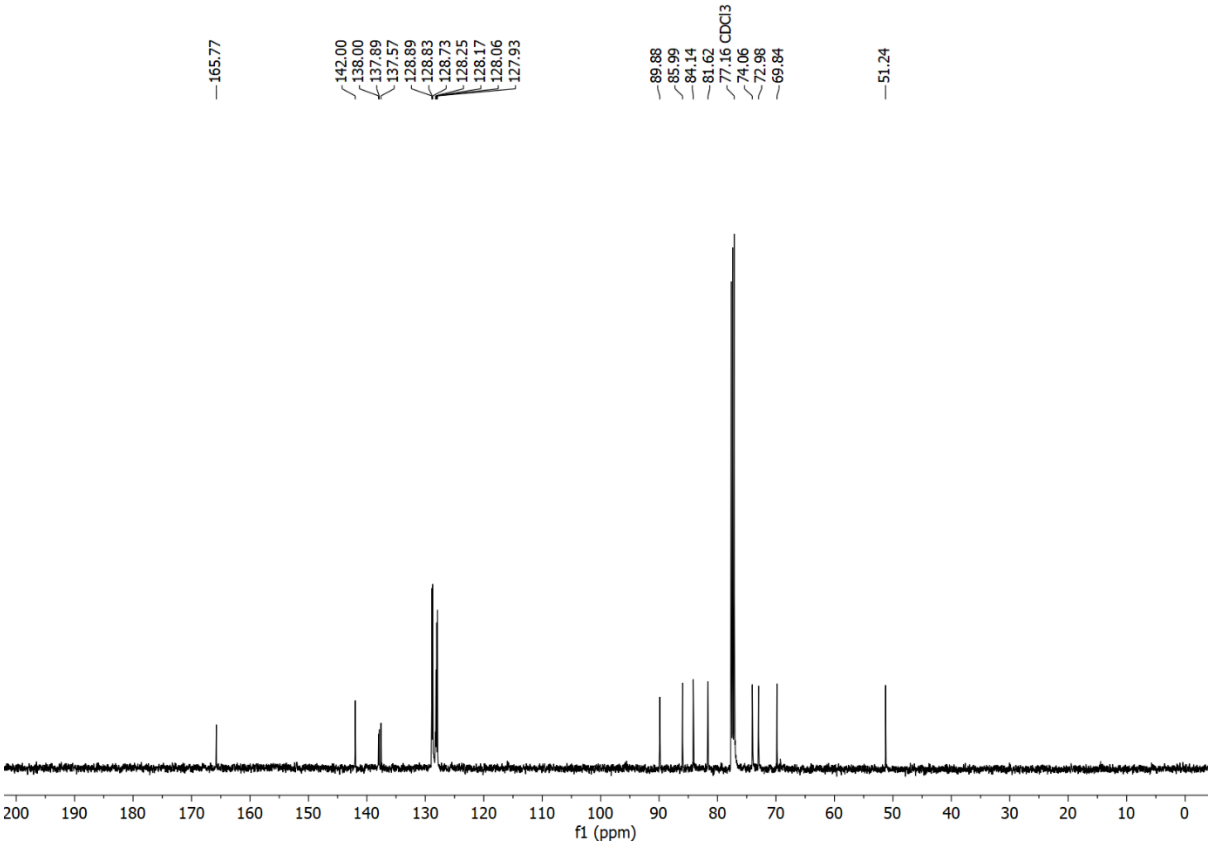

^{1}H-NMR (500 MHz, $CDCl_3$) and ^{13}C NMR (126 MHz, $CDCl_3$)

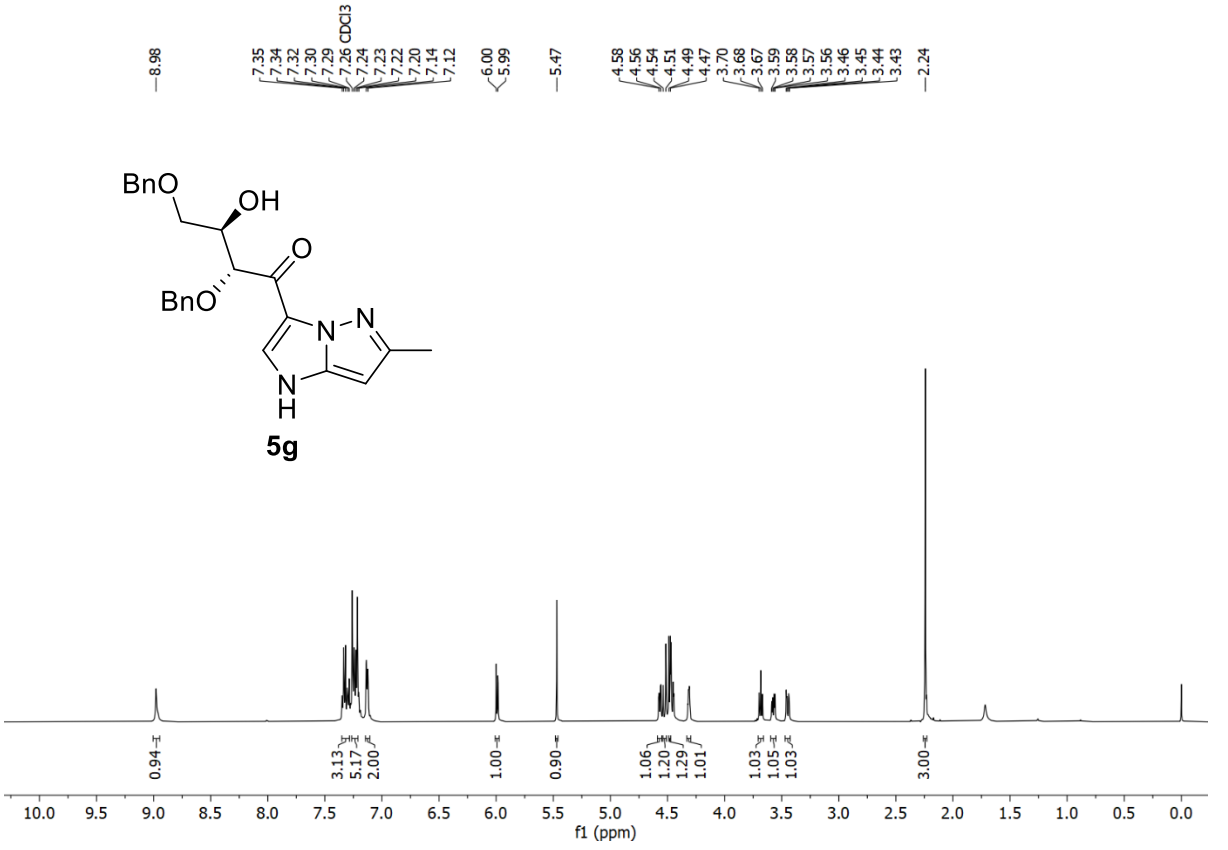

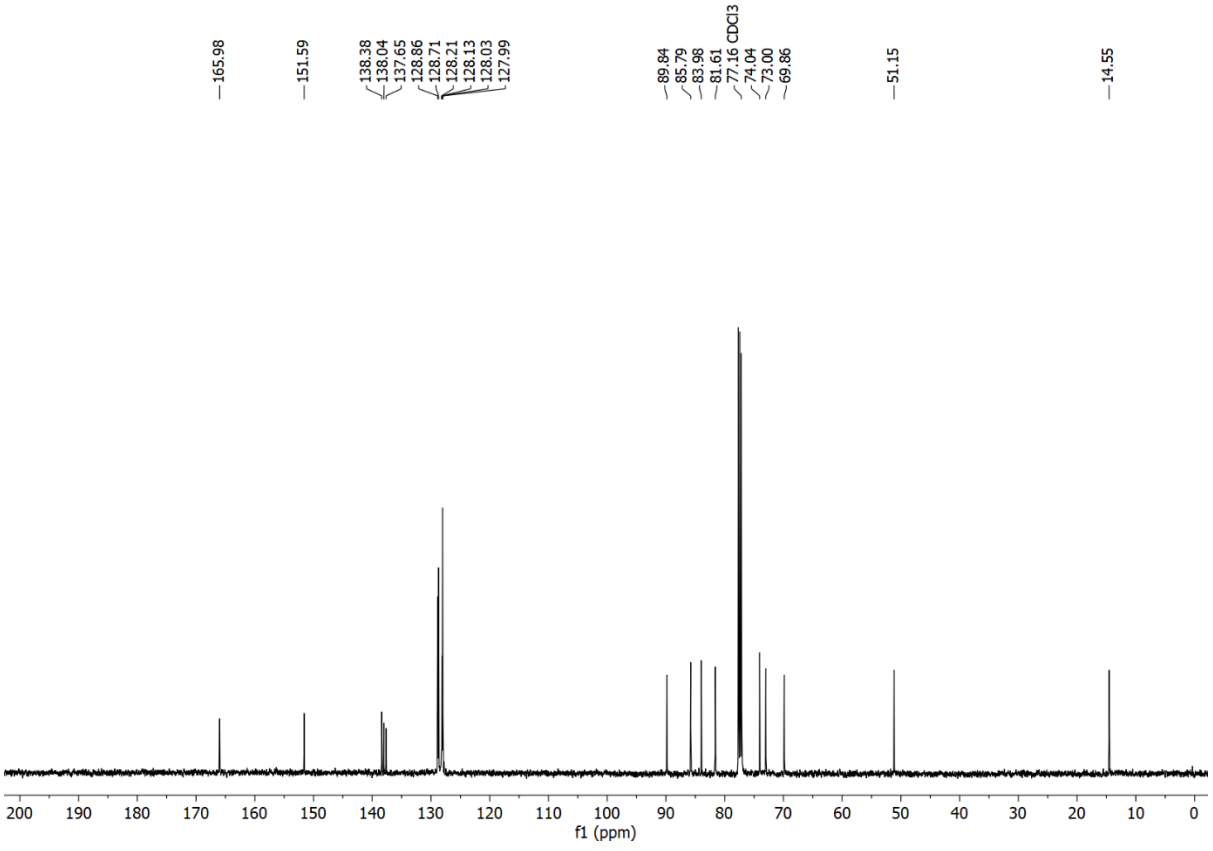

^{1}H-NMR (500 MHz, $CDCl_3$) and ^{13}C NMR (126 MHz, $CDCl_3$)

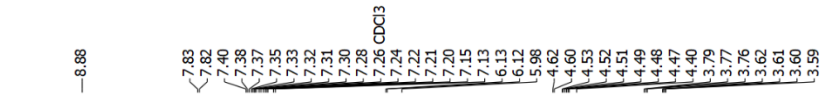

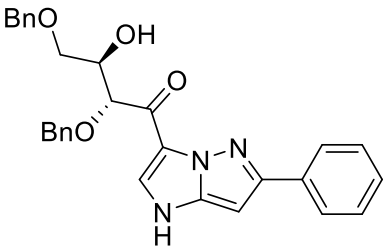

5h

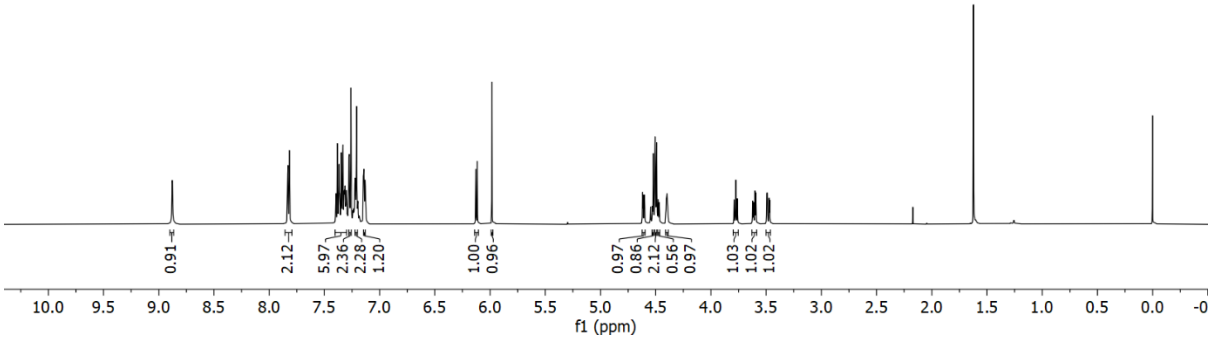

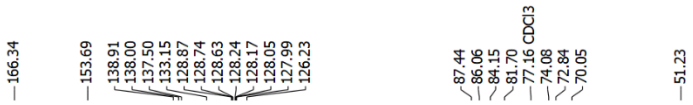

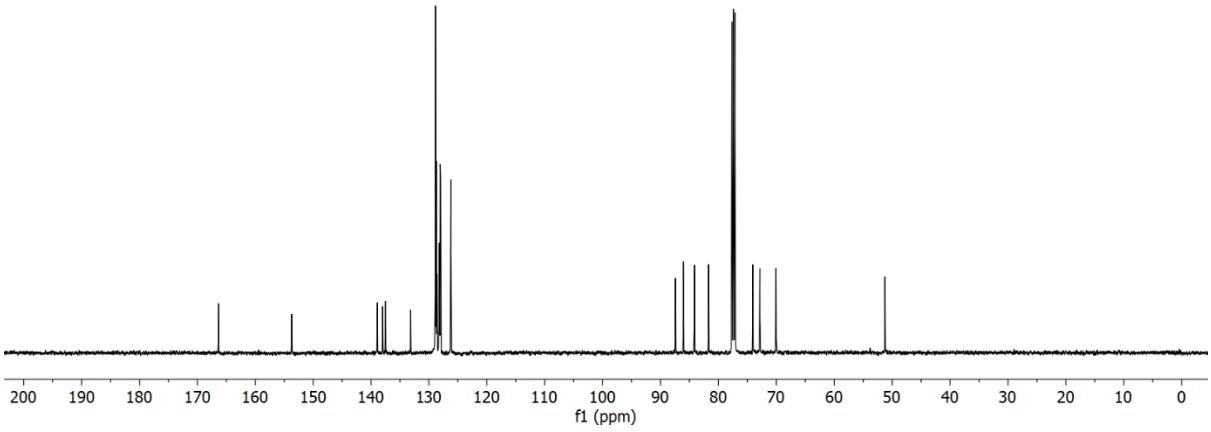

^{1}H-NMR (500 MHz, $CDCl_3$) and ^{13}C NMR (126 MHz, $CDCl_3$)

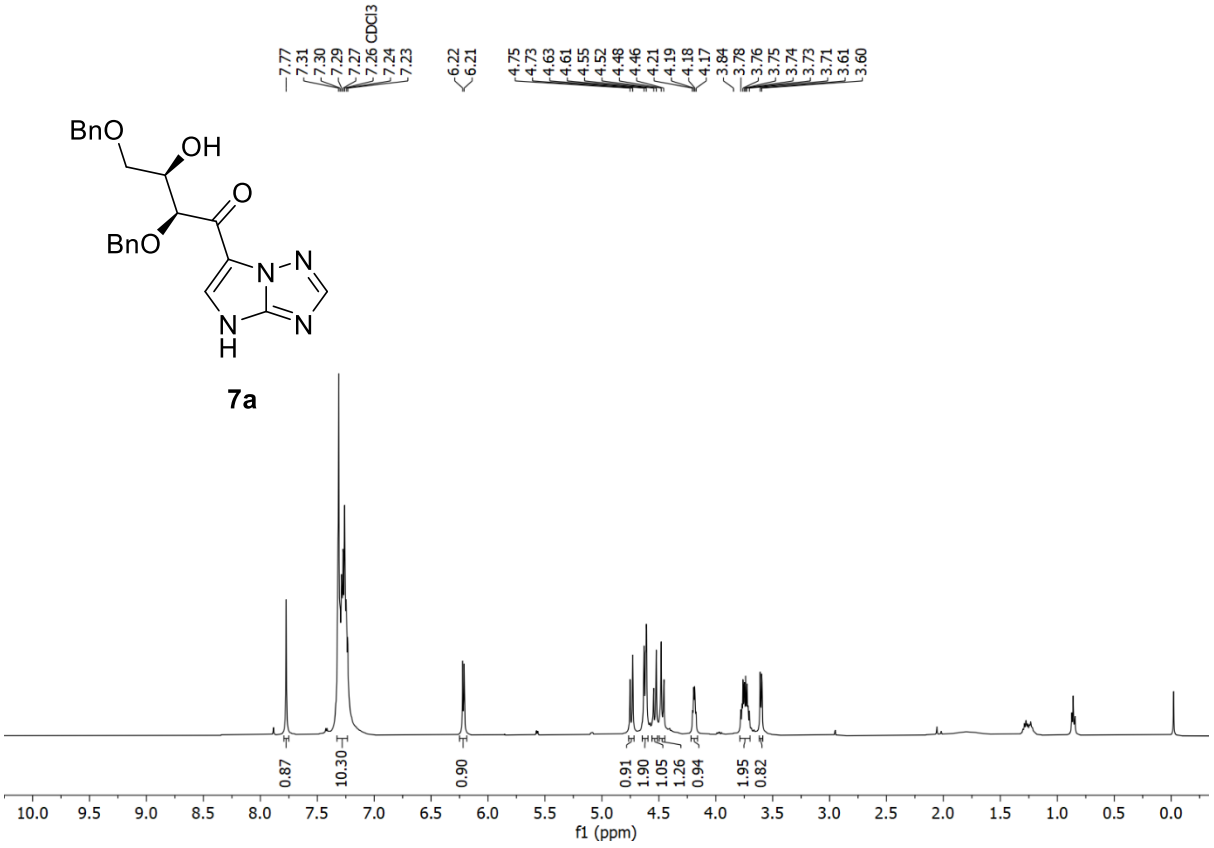

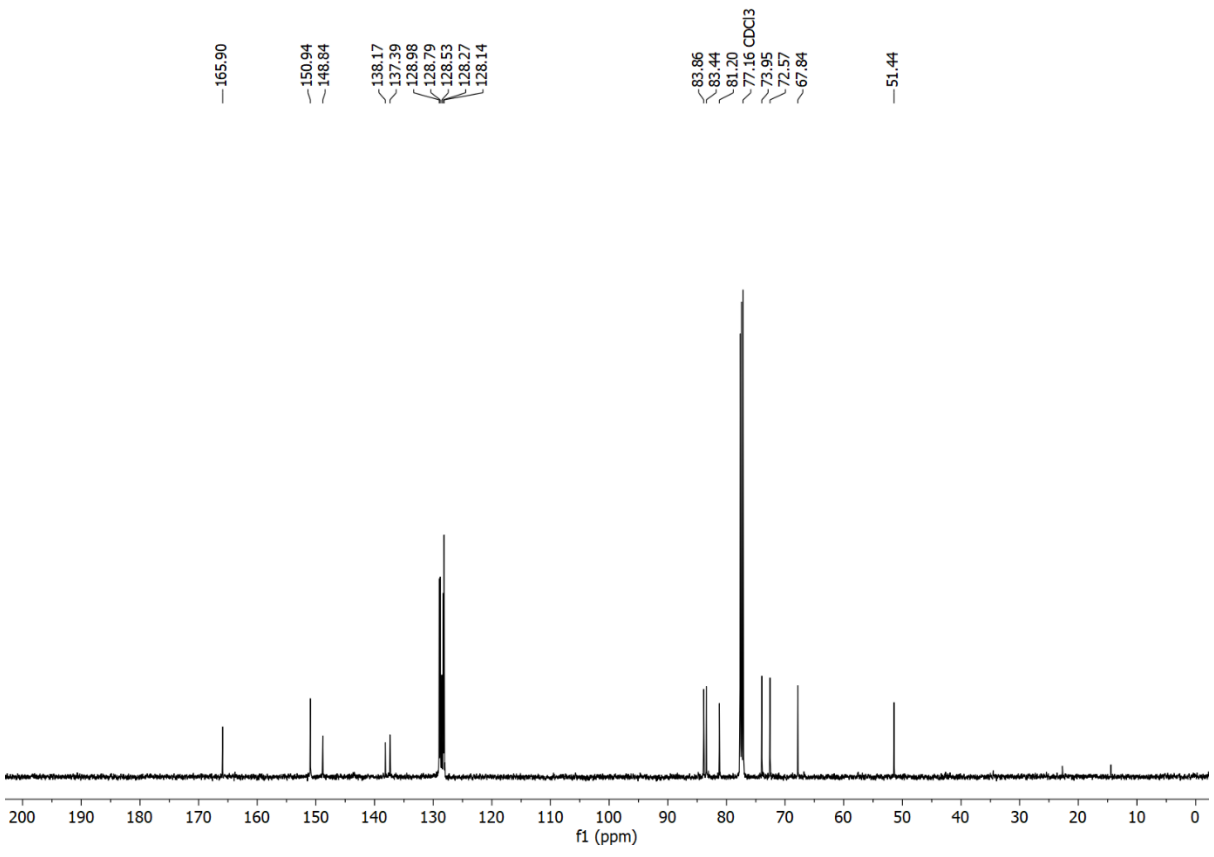

^{1}H-NMR (500 MHz, $CDCl_3$) and ^{13}C NMR (126 MHz, $CDCl_3$)

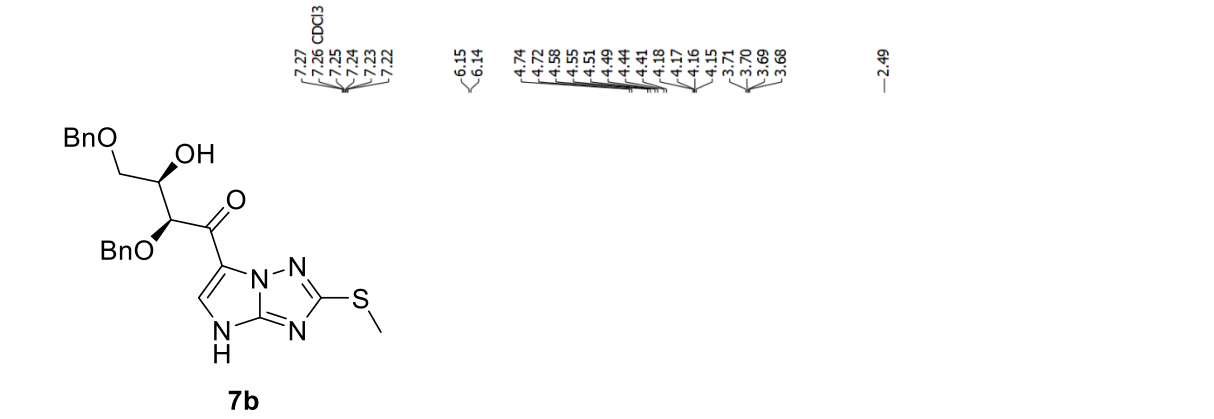

7b

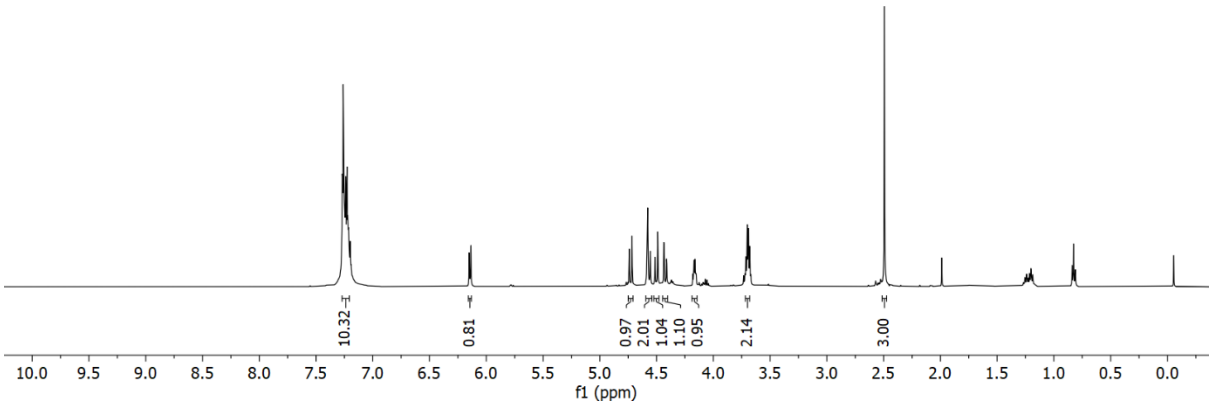

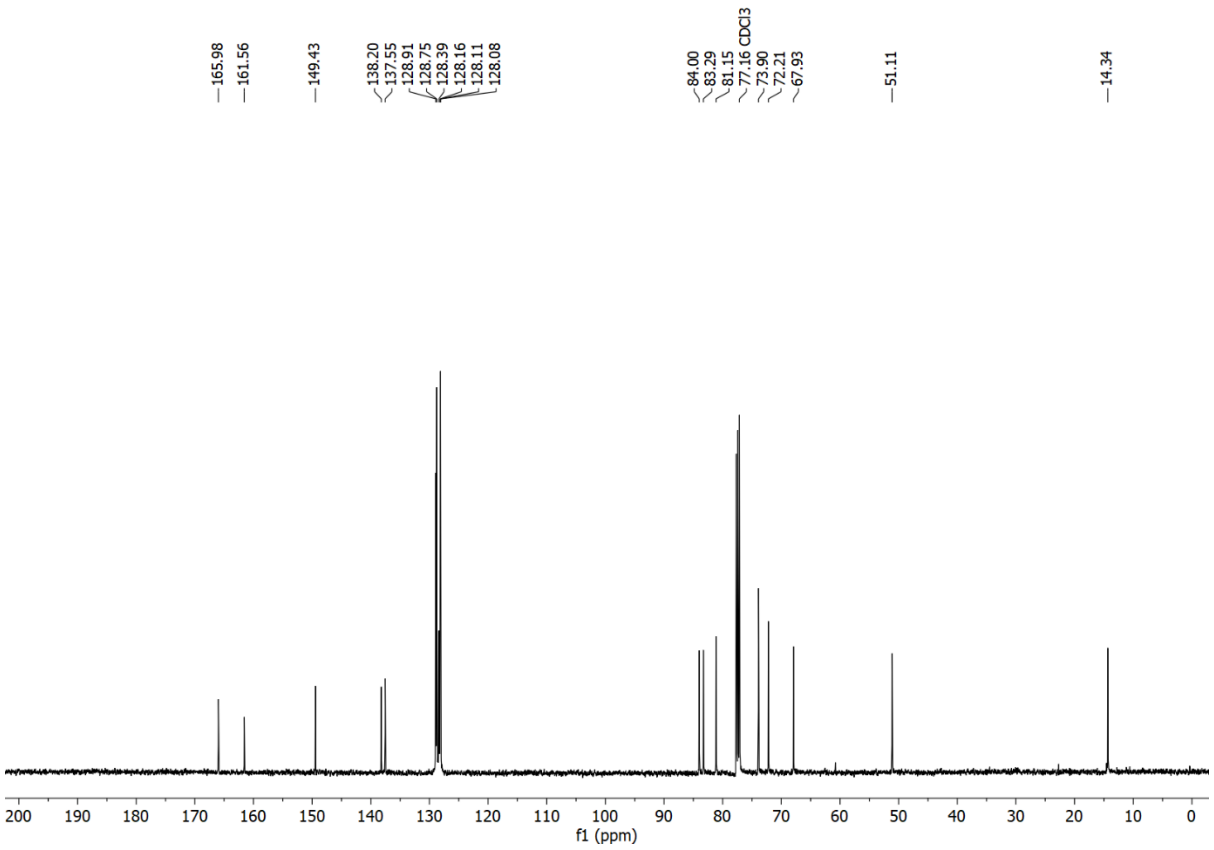

^{1}H-NMR (500 MHz, $CDCl_3$) and ^{13}C NMR (126 MHz, $CDCl_3$)

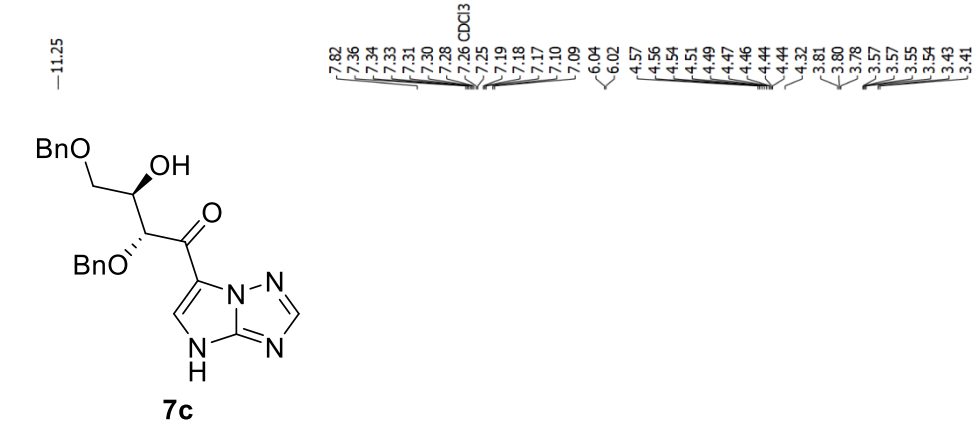

7c

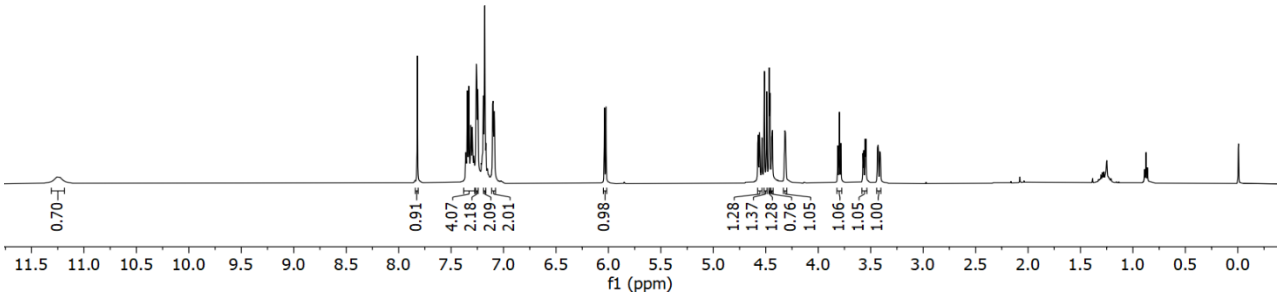

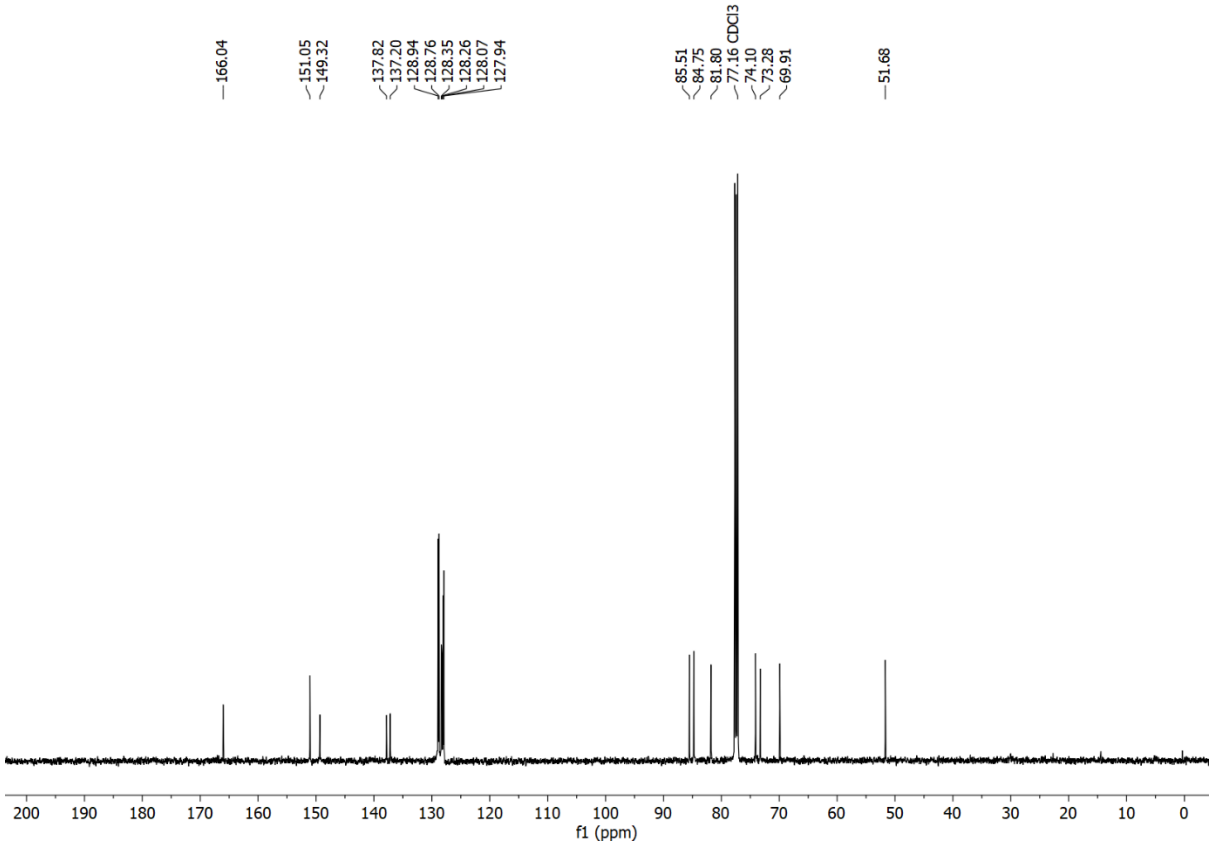

^{1}H-NMR (500 MHz, $CDCl_3$) and ^{13}C NMR (126 MHz, $CDCl_3$)